Molecular junctions based on aromatic coupling

SONGMEI WU[1], MARIA TERESA GONZÁLEZ[1], ROMAN HUBER[1], SERGIO GRUNDER[2], MARCEL MAYOR[2,3]*, CHRISTIAN SCHÖNENBERGER[1] AND MICHEL CALAME[1]*

[1]Department of Physics, University of Basel, Klingelbergstrasse. 82, CH-4056 Basel, Switzerland
[2]Department of Chemistry, University of Basel, St Johanns-Ring 19, CH-4056 Basel, Switzerland
[3]Forschungszentrum Karlsruhe GmbH, Institute for Nanotechnology, PO Box 3640, D-76021 Karlsruhe, Germany
*e-mail: marcel.mayor@unibas.ch; michel.calame@unibas.ch

Published online: 17 August 2008; doi:10.1038/nnano.2008.237

If individual molecules are to be used as building blocks for electronic devices, it will be essential to understand charge transport at the level of single molecules. Most existing experiments rely on the synthesis of functional rod-like molecules with chemical linker groups at both ends to provide strong, covalent anchoring to the source and drain contacts. This approach has proved very successful, providing quantitative measures of single-molecule conductance, and demonstrating rectification and switching at the single-molecule level. However, the influence of intermolecular interactions on the formation and operation of molecular junctions has been overlooked. Here we report the use of oligo-phenylene ethynylene molecules as a model system, and establish that molecular junctions can still form when one of the chemical linker groups is displaced or even fully removed. Our results demonstrate that aromatic $\pi-\pi$ coupling between adjacent molecules is efficient enough to allow for the controlled formation of molecular bridges between nearby electrodes.

To determine the electronic properties of molecular junctions[1–3] it is necessary to wire a single molecule (or a few molecules) between a source and drain electrode. This has become possible only in the last decade thanks to the development of new experimental techniques that allow the controlled formation of nanometre-sized gaps between pairs of metal electrodes[4–8]. These techniques provide a configuration with long-term stability and mechanical control of the gap size at the picometre scale, which allows reproducible measurements to be made[5,9].

Among these techniques, the construction of mechanical break junctions has attracted much attention[10–18]. In this approach, a gold wire with a constriction in its centre is continuously stretched, causing the diameter at the constriction to become smaller and smaller until the wire breaks to produce two atomic-scale gold contacts[19]. Molecules with two terminal anchor groups can then be anchored in the gap between the contacts to form a molecular junction (Fig. 1a).

Thiols (–SH) have been widely used as terminal anchor groups. Because the covalent gold–sulphur bond is stronger than a gold–gold bond[20,21], the gold atoms migrate to the ends of the contacts to form elongated tips when the electrodes are pulled apart (red arrows in Fig. 1b). This process continues until the force exceeds the strength of the gold–gold bond and the molecular junction breaks open. The electrical conductance G ($G = I/V$, where I is the current through the junction and V the applied voltage bias) of the junction remains approximately constant as the electrodes are pulled apart during stretching, but it drops suddenly when the junction breaks open.

For molecules with only one anchor group rather than two, one would not expect a stable metal–molecule–metal junction, because the molecules can only attach to one side of the junction (Fig. 1c). However, this assumption ignores intermolecular interactions and, as we shall see, these interactions can be relevant to the behaviour of molecular junctions.

CONDUCTANCE OF MOLECULAR JUNCTIONS

We used oligo-phenylene ethynylene (OPE) molecules as our model system. Conjugated molecules such as OPE have interesting electron transport properties due to the delocalization of electrons along the molecular backbone[22,23]. Such a structure results in the energy gap between the lowest unoccupied molecular orbital (LUMO) and the highest occupied molecular orbital (HOMO) being smaller (~3 eV) than the HOMO–LUMO gap of saturated molecules (~7 eV), leading to more efficient charge transport through the molecule.

We used a mechanically controllable break junction (MCBJ) setup to form molecular junctions in liquid (see Fig. 2 and Methods for further details)[24,25]. The electrical conductance was measured while opening the junction. Representative opening curves are shown in the solvent (Fig. 2d) and the same solvent but with added OPE–dithiol molecules (Fig. 2e). We present the electrical data on a logarithmic scale, because only the $\log G(z)$ representation yields a full view of the evolution of the conductance G during opening of the junction[17]. We first discuss $G(z)$ for the pure solvent (THF/mesitylene = 1:4 v/v ratio) (Fig. 2d).

When the substrate is bent, the gold bridge is stretched and $G(z)$ decreases. However, the decrease evolves as a series of conductance plateaus for G values above the quantum conductance unit $G_0 \equiv 2e^2/h$ (see top arrow in Fig. 2d). There is a so-called 'last plateau', with a value of $G \approx G_0$. This last plateau corresponds to a single-atom gold bridge. If the junction is elongated further, it

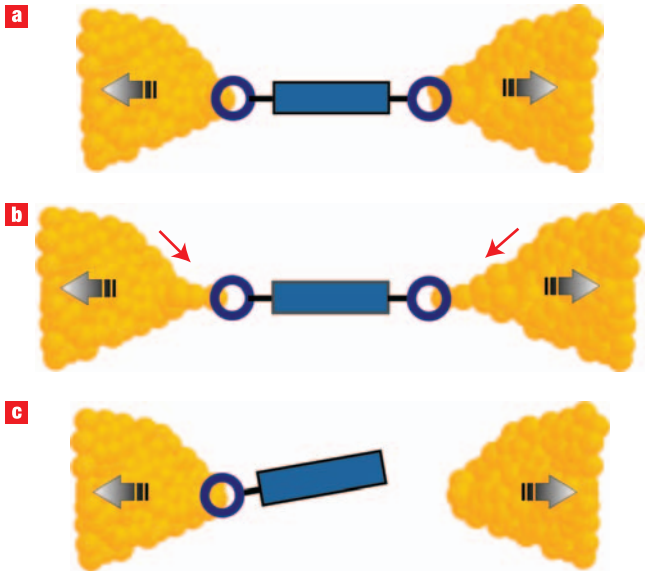

Figure 1 Anchoring of a molecule in a metal junction. a, A stable molecular junction is realized when a molecule (blue rectangle) anchors between the gold metal electrodes (orange) with the aid of two chemical linker groups (emphasized with circles) that form chemical bonds with the gold. **b**, When the electrodes are moved apart, the gold atoms are pulled by the anchored molecule into the periphery of the gold junctions (red arrows), leading to the formation of tips. **c**, Molecules with only one anchor group are not expected to form a stable molecular bridge.

breaks. Then, a sudden decrease of G is evident in the $G(z)$ curves. This is thought to be caused by a sudden rearrangement of the gold atoms, reshaping the front end of the two gold electrodes. The down-jump typically stops at a value of $G \approx 10^{-3}\,G_0$, when electron tunnelling between the electrodes sets in (see bottom arrow in Fig. 2d). Electron tunnelling with a constant tunnelling barrier height results in a linear dependence of $\log(G)$ versus z, as observed in the measurements. Because single curves vary and display fluctuations, we built histograms of the measured $\log(G)$ values (right side of Fig. 2d). Although measured in a solvent, this behaviour would look similar in vacuum. Hence, the solvent is a passive element in this reference experiment[24].

When OPE–dithiol molecules (having terminal –SH linkers on both ends) were added to our MCBJ liquid cell, the $G(z)$ dependence was markedly changed (Fig. 2e). Instead of a sudden drop followed by a tunnelling slope, as is observed in the solvent when the junction opens, clear conductance plateaus appear at G values below G_0, typically at $G \approx 10^{-4}G_0$. This is the signature of the formation of a molecular junction. The chance of formation is not unity, but amounts to the reasonably large fraction (40–50%) in this case. Because the plateaus are relatively noisy, the single-molecule conductance data display a broad, but very pronounced peak in the $\log(G)$ histogram (right side of Fig. 2e). From this peak we deduce $G = 1.2 \pm 0.1 \times 10^{-4}G_0$ for the single-molecule conductance value of the OPE–dithol molecule (see Methods). We emphasize that we always use all measured curves in our analysis. Curves that do not show plateaus contribute to a tunnelling background similar to that for the pure solvent[17].

MODIFYING ONE ANCHOR GROUP

The molecules (**1**–**5**) displayed in Table 1 were designed and synthesized for the charge transport characterization reported here. The table also illustrates the strategy of the present study. Using three-phenyl-ring OPE molecules, we gradually changed the strength of the molecular linker on one end of the molecule. Molecule **1** is our reference OPE–dithiol molecule, which has two terminal thiol anchors to covalently bridge the two contact electrodes. This molecule does form single-molecule junctions[26]. In molecule **2**, a pyridine–nitrogen atom on the *para* position of the terminal phenyl ring replaces the thiol anchor group. Here, one may still expect the formation of single-molecule junctions, due to the coordination of the nitrogen atom with the gold electrode[20,27,28]. In molecule **3**, the nitrogen atom is "hidden" by shifting it from the *para* to *ortho* position within the phenyl ring, which should drastically reduce the binding properties of the molecule[20]. Finally, the second anchor group is completely removed in **4**. Molecule **5** is a shorter derivative and serves as an additional control to complete the series.

The results of the corresponding conductance measurements are shown in Fig. 3. The order of molecules is similar to that in Table 1. It is immediately evident that in all cases a pronounced conductance peak appears. It is suprising that both the height and the width of these peaks are similar for molecules **1**–**4**. Going through the sequence from above, we see that the conductance value G_{peak}, corresponding to the peak position in the $\log(G)$ histogram, is for molecule **2** slightly reduced by a factor of approximately 2–3 compared with molecule **1**. This lower value could be explained by a weaker electronic coupling between the nitrogen and gold atoms. Recent studies show a strong dependence of conductance on the coordination of pyridine–nitrogen anchoring groups to the gold electrodes[28].

Although we expect a peak in $\log(G)$ for molecule **2**, a similar peak of equal magnitude for molecule **3** comes as a surprise. Because the nitrogen atom of the pyridine structure in molecule **3** is 'hidden', it may provide, if at all, a much less probable binding site to the electrode. In contrast to this, the identical magnitude and width of the peak in $\log(G)$ suggest that molecule **3** also binds in the junction with a similar probability as molecules **1** and **2**. Hence, the observed strong binding must have another origin. This is supported further by the measurements for molecule **4**. Although the anchor group at one end is now removed, we obtain very similar results for **3** and **4**. Why does a molecular junction form, even with molecular rods having only a single linker group on one side of the rod?

AROMATIC STACKING

We believe that the connection between the electrodes is made possible by a π–π stacking interaction between a pair of molecules[29–31]. If one molecule is anchored by means of its thiol linker group on, for example, the left electrode, another one bound to the right electrode can complete the mechanical assembly of the junction through π–π coupling through the phenyl rings. This interpretation is supported by the shift of G_{peak} to lower values by more than an order of magnitude. In this picture, a reduced G value is expected, because the pair of molecules will be longer than a single dithiol molecule anchored between gold electrodes. We observe that the junctions form with a similar probability, whether for dithiolated compounds or monothiolated compounds. This might *a priori* appear surprising, because the molecular junctions formed by monothiolated compounds will be composed of two molecules and might therefore occur less frequently. However, this is not the case, as we do not have a diffusion-limited experimental situation. After immersion in the molecular solution (0.25 mM, see Methods), the gold bridge will be covered with a monolayer of molecules over its whole surface. Upon breaking open the gold

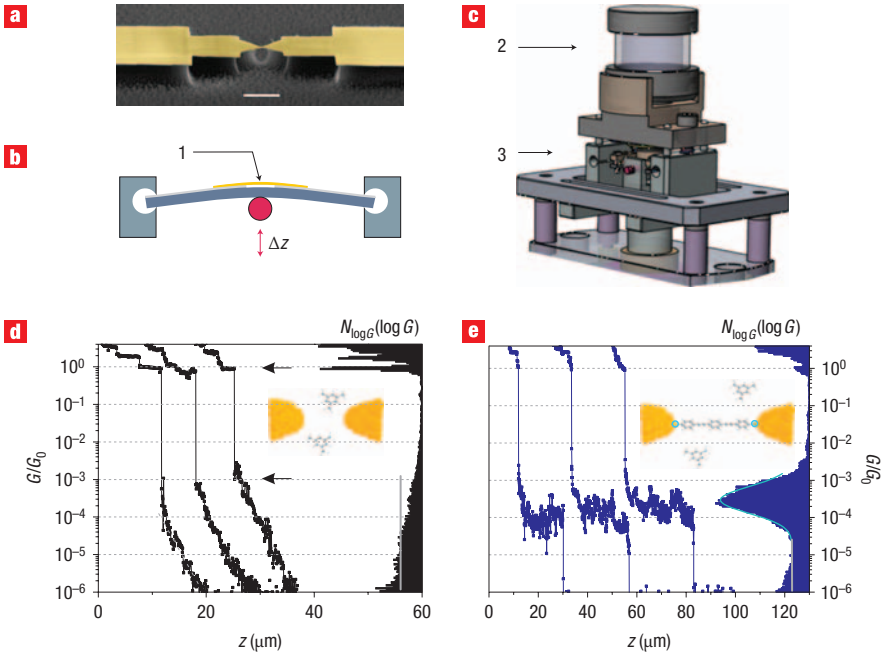

Figure 2 Measurement apparatus and conductance curves. a, Scanning electron microscopy (SEM) image of a typical sample used in this mechanically controlled break junction (MCBJ) apparatus. The top part (yellow) is made from gold. The gold structure has a constriction at its centre and is fabricated by electron-beam lithography on a flexible steel plate that includes an insulating polyimide top layer. After plasma etching, the gold constriction forms a suspended bridge. (Scale bar, 1 μm). **b**, The sample is mounted in a mechanical bending apparatus in which a pushrod is pressing from below against the flexible sample. An upward pushrod movement Δz increases the bending of the substrate. As a consequence, an increasing pulling force is established at the constriction of the gold electrode structure (1). The gold bridge elongates and finally breaks in the narrowest section. **c**, The actual MCBJ setup also embodies a liquid cell (2) on top of the sample holder (3). **d**, **e**, Three typical single $G(z)$ curves measured in pure solvent (**d**, black) and in the same solvent but with added OPE–dithiol molecules (**e**, blue). The curves are shifted horizontally for clarity. The two black arrows in **d** indicate respectively the breaking point of the gold junction at $G \approx G_0$ (top arrow) and the onset of the tunnelling regime at $G \approx 10^{-3}G_0$ (bottom arrow). Also shown are histograms ($N_{\log G}(\log G)$) of $\log(G)$ values obtained from 100 opening curves each. In the tunnelling regime, the solvent contribution results in a constant number of counts in the histogram (vertical grey lines). In the presence of OPE–dithiol molecules a clear peak signature develops from which we deduce the molecular junction conductance (Gaussian fit).

Table 1 The molecules investigated and related parameters. The molecular rods 1–5 were synthesized in their acetyl-protected form (R = $COCH_3$). *In situ* deprotection formed the free thiol, which bound with the gold electrodes (R = Au). The different anchoring groups are highlighted with a blue circle. Lp refers to the nitrogen lone pair and H_t denotes the terminal hydrogen. The length of each molecule is obtained after energy minimization using the MM2 force field (ChemDraw 3D). The single-molecule conductance value G was deduced from the peak that appears in the log(G) histograms of 100 opening $G(z)$ curves obtained from three to four different samples.

	Molecule	Length, L (Å)	No. of samples	Conductance, G (G_0)
1	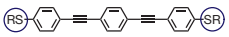	20.7 (S–S)	4	$(1.2 \pm 0.1) \times 10^{-4}$
2	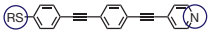	18.7 (S–N) 19.4 (S–Lp)	3	$(5.7 \pm 2.4) \times 10^{-5}$
3	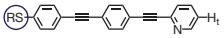	19.8 (S–H_t)	3	$(6.6 \pm 1.3) \times 10^{-6}$
4	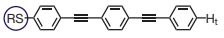	19.8 (S–H_t)	3	$(5.9 \pm 2.4) \times 10^{-6}$
5	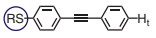	12.9 (S–H_t)	4	—

bridge, there will be a high local concentration of molecules available for the formation of a molecular junction. Although the kinetics of junction formation will depend on whether we have dithiolated or monothiolated compounds, the typical time constants will be orders of magnitude faster than can be resolved by our experimental setup (typically 5 ms). We therefore do not expect to see a difference between the two situations.

As the strength of π–π stacking depends strongly on the conjugation extent of the system and the overlap between adjacent compounds, one straightforward control experiment, without modifying to a great extent the electronic structure of the molecules (see Supplementary Information, Fig. S1), is to investigate an OPE compound with only two phenylene units (molecule **5**). Here, the width of the conductance peak in the log(G) histogram is much broader than shown before by any other molecule (Fig. 3). Although this peak is also somewhat shallow, single $G(z)$ curves still display clearly visible but noisier plateaus at values larger than the plateau values for molecules **3** and **4** (see Supplementary Information, Fig. S2). We believe that the peak for molecule **5** is less pronounced because of the reduced π–π interaction for these shorter molecules, leading to a mechanically less stable junction. Note that a pair of molecules of **5** tends to

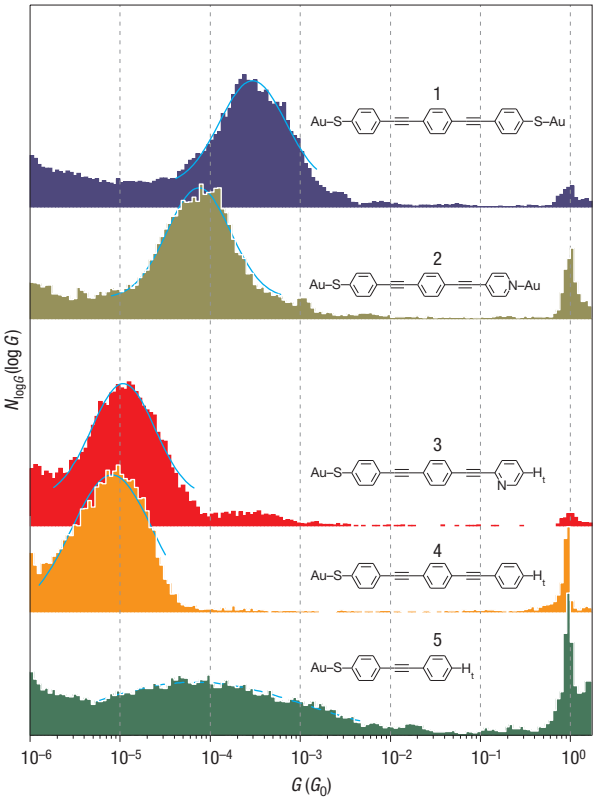

Figure 3 Conductance histograms for the different molecules. Comparison of log(G) histograms for OPE molecules with two linking terminals (molecules **1** and **2**), and with only one thiol linker (molecules **3** to **5**). Each histogram was built from 100 conductance traces obtained during successive opening cycles, similar to the example shown in Fig. 2e. The pronounced Gaussian-like peaks (solid lines) in the log(G) histograms represent the signatures of the specific molecule investigated. The molecular junction conductance is deduced from the peak conductance G_{peak}.

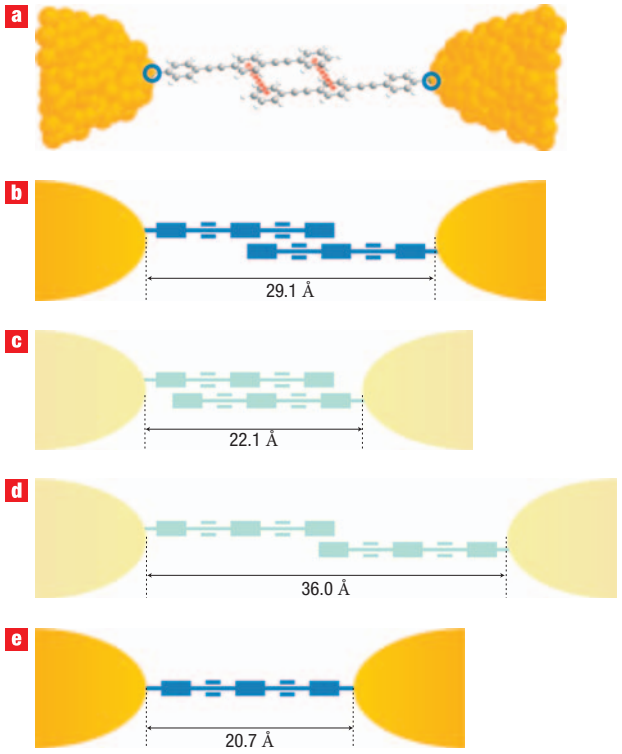

Figure 4 Illustration of possible stacking configurations. a, Staggered $\pi-\pi$ stacking configuration of a pair of OPE–monothiol molecules within which the aromatic rings are shifted by half of the ring length. **b**–**e**, Simplified representation of different configurations of OPE molecules between the electrodes, where a rectangle indicates a phenyl ring: the configuration anticipated as the most probable one (**b**); less probable configurations due to steric hindrance (**c**) and reduced conjugation and overlap (**d**); junction distance between the sulphur atoms for a single OPE–dithiol molecule between electrodes (**e**). All distances are taken between the sulphur atoms on either side and were estimated after minimizing the energy of the compound using a molecular mechanics calculation using the MM2 force field (ChemDraw 3D).

have a higher conductance value than a pair of molecules of **4** because of the reduced distance the electrons have to tunnel between the gold electrodes through the molecular bridge. We also emphasize that without deprotecting the thiol function (see Methods), no molecular signature can be detected in the break junction. This permits the elimination of other unanticipated interactions except for intermolecular interactions to explain the signal observed for compounds **3**–**5**. Finally, we also checked that for compounds where no aromatic stacking is possible, such as in monothiolated alkane chains, we do not observe the formation of molecular junctions (see Supplementary Information, Fig. S3). These experiments clearly reveal the importance of the immediate surroundings in transport molecular junctions involving a single molecule or a few molecules[32–35].

TUNNELLING PICTURE

As briefly stated above, the different conductance values can be qualitatively attributed to the difference in the distance that electrons have to tunnel between the gold electrodes. This distance is determined by the length of a single molecule if there are anchors on both sides, or by the length of a $\pi-\pi$ stacked pair of molecules otherwise. The stacking of a pair of monothiol molecules **3** is illustrated in Fig. 4a. Figure 4b–d presents different stacking configurations of the same molecule, and Fig. 4e shows the two-side anchored dithiol molecule.

By considering the σ-framework and the π-electrons separately, Hunter and Sanders[36] emphasized that the geometrical arrangement of interacting aromatic molecules is essentially governed by electrostatics. Two aromatic molecules brought in close proximity will not register directly on top of each other due to the electrostatic repulsion of the negative π-electron clouds. A net positive interaction will result from the $\pi-\sigma$ attraction, translating for instance as a staggered face-to-face configuration as shown in Fig. 4a. The question of the relative orientation of the aromatic rings within an OPE molecule remains a matter of debate. The fully planar configuration has the minimum energy[32,37,38]. However, in diluted solution at room temperature, experiments and calculations suggest that the aromatic rings of OPE molecules are able to explore different orientations[37,39]. This is certainly true at low concentration. At higher concentrations, where the $\pi-\pi$ interaction induces aggregation, coplanar stacking appears favoured[38,40,41]. This is also the case in crystals of similar aromatic compounds[42,43]. In our case, the molecules self-assemble at the surface of the gold electrodes, leading to a high local concentration. We therefore expect the molecules to form coplanar stacks as illustrated in Fig. 4a. Figure 4b–d depicts

possible stacking configurations. We believe that Fig. 4b represents the actual stacking configuration of a pair of molecules **4**. The structures in Fig. 4c,d are seen as less probable because of steric hindrance and because of the weaker $\pi-\pi$ interaction due to the reduced overlap between the molecules.

In a simple tunnelling picture where electrons tunnel through an effective medium over a distance d, the conductance G can be written as $G = Ae^{-\beta d}$. The decay constant β is determined by the electronic parameters of the effective medium (here, the molecules). For a given electrode material (here, gold), the pre-factor A depends on the electron density-of-states at the point where the molecule contacts the gold electrode. Because this is determined by thiol anchors both in a single molecule and a stacked pair of molecules, this factor can be taken as a constant. Note that in this tunnelling picture, the symmetric and constant peak widths in the log(G) histograms (Fig. 3) reflect the fact that the conductance fluctuations mainly arise due to variations in the exponent of the conductance. The conductance fluctuations can therefore be attributed to variations of the effective tunnelling distance d and the decay constant β, as generated by local changes in the geometrical arrangement of the molecular junction. Experimental and theoretical evidence has already been provided for a strong through-space conjugation between π-systems held together by carbon linkers[44]. For the following estimate we will use a typical average decay constant of 0.3 Å^{-1} for the OPE derivatives as obtained from electron transfer rates in donor–bridge–acceptor systems[45–47] and theory[48,49]. The distances between the two sulfur atoms are 20.7 Å for the single OPE dithiol molecule (Fig. 4e) and 29.1 Å for a pair of OPE–monothiols (Fig. 4b). The longer tunnelling distance between electrodes for a stacking junction leads to a 12 times lower conductance. This is in reasonable agreement with experiment, which shows a 20-fold difference.

In conclusion, we have demonstrated that an intermolecular $\pi-\pi$ stacking interaction between monothiol molecules composed of alternating phenylene and ethynylene units is strong enough to induce the formation of molecular junctions. The yield is similar to that of dithiol molecules, with a molecular signature reaching the same degree of quality as judged from the statistical variation of single junction conductance values. This is a significant finding for molecular electronics. Intermolecular aromatic stacking plays a determinant role in stabilizing nano-objects. The importance of $\pi-\pi$ overlap has long been recognized in thin-film organic electronics, molecular mechanics, and especially in biomolecular and supramolecular chemistry. We show here that $\pi-\pi$ stacking can also be used as the dominant guiding force for the formation of molecular bridges in few-molecule electronic junctions. These experimental findings provide a strong basis for the design of future electromechanical and sensing devices operating at the single-molecule level.

METHODS

SAMPLE STRUCTURE AND MCBJ APPARATUS

The gold structure was fabricated by electron-beam lithography on a flexible spring steel plate substrate onto which an insulating polyimide layer, several micrometres thick, was cast, followed by the evaporation of a thin adhesion layer of titanium of thickness 10 nm at an angle of ~50° and the evaporation of a 60 nm gold layer perpendicular to the sample. This procedure ensures good adhesion of the gold layer but avoids titanium in the central region of the bridge. The bridge was typically 150 nm in width and 200–300 nm in length. The bridge was suspended by etching the polyimide in an oxygen plasma. Thereafter, the sample was mounted in a mechanical bending apparatus (MCBJ apparatus). The mechanical design provided a large attenuation between the variation in the vertical pushrod movement Δz and the respective variation in the gap distance Δd. The attenuation factor $a = \Delta d/\Delta z$ was found to be in the range $1.6–4 \times 10^{-5}$. The pushrod was driven by a micrometre screw and a gear box by a stepper motor at a velocity of $v_z = 30\ \mu m\ s^{-1}$, so that the two gold leads separated at 0.5–2.0 nm s^{-1}. The pushrod was periodically moved upwards and downwards. In this way the gold junction could be opened and closed many times, and the conductance measured, resulting in so-called opening and closing curves. In the present work we discuss only data obtained from opening curves. Because many opening curves can be acquired, a statistical analysis is possible.

In our MCBJ setup, a glass liquid cell was gently pressed against the sample from above through a soft viton tube in order to immerse the suspended gold bridge in liquid. The molecular rods **1**–**5** were synthesized with acetyl-protected thiol anchor groups. To assess the conductance G of a particular molecule, the junction was periodically opened and closed in the presence of a 0.25 mM solution of molecules **1**–**5** in a 3 ml mixture of THF/mesitylene (1:4 v/v ratio) (henceforth the solvent) to which 30 μM tetrabutyl ammonium hydroxide (TBAH) was added to remove the acetyl protection groups *in situ*. During the measurements, the solution was kept under an argon atmosphere to prevent the de-protected bifunctional molecules from polymerization through disulphide bond formation.

ELECTRICAL MEASUREMENTS AND ANALYSIS

A bias voltage of 0.2 V was applied between the left and right gold electrodes and the resulting current measured with a custom-made current-to-voltage converter, which enabled measurement of conductance values ranging from the quantized conductance value of a single-atom contact $G_0 = 2e^2/h$ down to $\sim 1 \times 10^{-7} G_0$. The junction was opened until the conductance value G was below the resolution limit of our amplifiers and closed until a gold–gold contact was re-established, identified by $G > G_0$ ($\sim 10\ G_0$). During junction opening and closing, G was continuously recorded. In this work, 100 open–close cycles defined one set of measurement for each sample. For all molecules, at least three sets of measurements were taken, with each set acquired on a freshly prepared sample which had not been broken before. For each molecule the measured conductance values of all opening curves were analysed in a statistical manner by plotting the histogram of all values of the logarithm of G. The log(G) histogram displayed a pronounced peak from which we obtained the single-molecule G value. This value was deduced by fitting a Gaussian function on the overall peak and transforming it back from the log(G) scale to the linear G representation[26] (see Supplementary Information, Fig. S4, for histograms in the linear representation).

Received 12 March 2008; accepted 16 July 2008; published 17 August 2008.

References

1. Ratner, M. A. & Aviram, A. Molecular rectifiers. *Chem. Phys. Lett.* **29,** 277–283 (1974).
2. Joachim, C., Gimzewski, J. K. & Aviram, A. Electronics using hybrid-molecular and mono-molecular devices. *Nature* **408,** 541–548 (2000).
3. Nitzan, A. & Ratner, M. A. Electron transport in molecular wire junctions. *Science* **300,** 1384–1389 (2003).
4. Joachim, C. & Ratner, M. A. Molecular electronics special feature: Molecular electronics: some views on transport junctions and beyond. *Proc. Natl Acad. Sci. USA* **102,** 8801–8808 (2005).
5. Selzer, Y. & Allara, D. L. Single-molecule electrical junctions. *Ann. Rev. Phys. Chem.* **57,** 593–623 (2006).
6. Tao, N. J. Electron transport in molecular junctions. *Nature Nanotech.* **1,** 173–181 (2006).
7. Lindsay, S. M. & Ratner, M. A. Molecular transport junctions: Clearing mists. *Adv. Mater.* **19,** 23–31 (2007).
8. Weibel, N., Grunder, S. & Mayor, M. Functional molecules in electronic circuits. *Org. Biomol. Chem.* **5,** 2343–2353 (2007).
9. Mantooth, B. & Weiss, P. Fabrication, assembly, and characterization of molecular electronic components. *Proc. IEEE* **91,** 1785–1802 (2003).
10. Reed, M. A., Zhou, C., Müller, C. J., Burgin, T. P. & Tour, J. M. Conductance of a molecular junction. *Science* **278,** 252–254 (1997).
11. Kergueris, C. *et al.* Electron transport through a metal–molecule–metal junction. *Phys. Rev. B* **59,** 12505–12513 (1999).
12. Smit, R. H. M. *et al.* Measurement of the conductance of a hydrogen molecule. *Nature* **419,** 906–909 (2002).
13. Reichert, J. *et al.* Driving current through single organic molecules. *Phys. Rev. Lett.* **88,** 176804 (2002).
14. Csonka, S. *et al.* Fractional conductance in hydrogen-embedded gold nanowires. *Phys. Rev. Lett.* **90,** 116803 (2003).
15. Böhler, T., Grebing, J., Mayer-Gindner, A., von Löhneysen, H. & Scheer, E. Mechanically controllable break-junctions for use as electrodes for molecular electronics. *Nanotechnology* **15,** S465–S471 (2004).
16. Champagne, A., Pasupathy, A. & Ralph, D. Mechanically adjustable and electrically gated single-molecule transistors. *Nano Lett.* **5,** 305–308 (2005).
17. González, M. T. *et al.* Electrical conductance of molecular junctions by a robust statistical analysis. *Nano Lett.* **6,** 2238–2242 (2006).
18. Lörtscher, E., Ciszek, J., Tour, J. & Riel, H. Reversible and controllable switching of a single-molecule junction. *Small* **2,** 973–977 (2006).
19. Agrait, N., Yeyati, A. L. & van Ruitenbeek, J. M. Quantum properties of atomic-sized conductors. *Phys. Rep.* **377,** 81–279 (2003).
20. Xu, B., Xiao, X. & Tao, N. Measurements of single-molecule electromechanical properties. *J. Am. Chem. Soc.* **125,** 16164–16165 (2003).

21. Huang, Z., Chen, F., Bennett, P. & Tao, N. Single molecule junctions formed via Au-thiol contact: Stability and breakdown mechanism. *J. Am. Chem. Soc.* **129,** 13225–13231 (2007).
22. James, D. K. & Tour, J. M. Molecular wires. *Top. Curr. Chem.* **257,** 33–62 (2005).
23. Weiss, E. A., Wasielewski, M. R. & Ratner, M. A. Molecules as wires: Molecule-assisted movement of charge and energy. *Top. Curr. Chem.* **257,** 103–133 (2005).
24. Grüter, L., González, M. T., Huber, R., Calame, M. & Schönenberger, C. Electrical conductance of atomic contacts in a liquid environment. *Small* **1,** 1067–1070 (2005).
25. Grüter, L. *et al.* Resonant tunnelling through a C_{60} molecular junction in a liquid environment. *Nanotechnology* **16,** 2143–2148 (2005).
26. Huber, R. *et al.* Electrical conductance of conjugated oligomers at the single molecule level. *J. Am. Chem. Soc.* **130,** 1080–1084 (2008).
27. Venkataraman, L. *et al.* Single-molecule circuits with well-defined molecular conductance. *Nano Lett.* **6,** 458–462 (2006).
28. Li, X.-L. *et al.* Thermally activated electron transport in single redox molecules. *J. Am. Chem. Soc.* **129,** 11535–11542 (2007).
29. Kim, K., Tarakeshwar, P. & Lee, J. Molecular clusters of π-systems: Theoretical studies of structures, spectra, and origin of interaction energies. *Chem. Rev.* **100,** 4145–4186 (2000).
30. Watson, M., Fechtenkotter, A. & Müllen, K. Big is beautiful – "aromaticity" revisited from the viewpoint of macromolecular and supramolecular benzene chemistry. *Chem. Rev.* **101,** 1267–1300 (2001).
31. Hoeben, F., Jonkheijm, P., Meijer, E. & Schenning, A. About supramolecular assemblies of π-conjugated systems. *Chem. Rev.* **105,** 1491–1546 (2005).
32. Taylor, J., Brandbyge, M. & Stokbro, K. Conductance switching in a molecular device: The role of side groups and intermolecular interactions. *Phys. Rev. B* **68,** 121101 (2003).
33. Blum, A. *et al.* Charge transport and scaling in molecular wires. *J. Phys. Chem. B* **108,** 18124–18128 (2004).
34. Selzer, Y. *et al.* Effect of local environment on molecular conduction: Isolated molecule versus self-assembled monolayer. *Nano Lett.* **5,** 61–65 (2005).
35. Galperin, M., Ratner, M. A. & Nitzan, A. Molecular transport junctions: vibrational effects. *J. Phys. Condens. Matter* **19,** 103201 (2007).
36. Hunter, C. A. & Sanders, J. K. M. The nature of π–π interactions. *J. Am. Chem. Soc.* **112,** 5525–5534 (1990).
37. Seminario, J., Zacarias, A. & Tour, J. Theoretical interpretation of conductivity measurements of a thiotolane sandwich. A molecular scale electronic controller. *J. Am. Chem. Soc.* **120,** 3970–3974 (1998).
38. Levitus, M. *et al.* Steps to demarcate the effects of chromophore aggregation and planarization in poly(phenyleneethynylene)s. 1. Rotationally interrupted conjugation in the excited states of 1,4-bis(phenylethynyl)benzene. *J. Am. Chem. Soc.* **123,** 4259–4265 (2001).
39. Okuyama, K., Hasegawa, T., Ito, M. & Mikami, N. Electronic-spectra of tolane in a supersonic free jet – large-amplitude torsional motion. *J. Phys. Chem.* **88,** 1711–1716 (1984).
40. Miteva, T., Palmer, L., Kloppenburg, L., Neher, D. & Bunz, U. Interplay of thermochromicity and liquid crystalline behavior in poly(p-phenyleneethynylene)s: π–π interactions or planarization of the conjugated backbone? *Macromolecules* **33,** 652–654 (2000).
41. Kim, J. & Swager, T. M. Control of conformational and interpolymer effects in conjugated polymers. *Nature* **411,** 1030–1034 (2001).
42. Li, H., Powell, D. R., Firman, T. K. & West, R. Structures and photophysical properties of model compounds for arylethynylene disilylene polymers. *Macromolecules* **31,** 1093–1098 (1998).
43. Wang, C., Batsanov, A., Bryce, M. & Sage, I. Nanoscale aryleneethynylene molecular wires with reversible fluorenone electrochemistry for self-assembly onto metal surfaces. *Org. Lett.* **6,** 2181–2184 (2004).
44. Seferos, D. S., Trammell, S. A., Bazan, G. C. & Kushmerick, J. G. Probing π-coupling in molecular junctions. *Proc. Natl Acad. Sci. USA* **102,** 8821–8825 (2005).
45. Creager, S. *et al.* Electron transfer at electrodes through conjugated "molecular wire" bridges. *J. Am. Chem. Soc.* **121,** 1059–1064 (1999).
46. Schlicke, B., Belser, P., De Cola, L., Sabbioni, E. & Balzani, V. Photonic wires of nanometric dimensions. Electronic energy transfer in rigid rodlike $Ru(bpy)^{32+}$-(ph)*n*-$os(bpy)^{32+}$ compounds (ph = 1,4-phenylene; $n = 3, 5, 7$). *J. Am. Chem. Soc.* **121,** 4207–4214 (1999).
47. Atienza, C. *et al.* Tuning electron transfer through p-phenyleneethynylene molecular wires. *Chem. Commun.* **30,** 3202–3204 (2006).
48. Magoga, M. & Joachim, C. Conductance and transparence of long molecular wires. *Phys. Rev. B* **56,** 4722–4729 (1997).
49. Tomfohr, J. K. & Sankey, O. F. Simple estimates of the electron transport properties of molecules. *Phys. Status Solidi* **233,** 59–69 (2002).

Supplementary Information accompanies this paper at www.nature.com/naturenanotechnology.

Acknowledgements

This work was financed by the Swiss National Science Foundation and the National Center of Competence in Research 'Nanoscale Science'. We also acknowledge the GEBERT RÜF STIFTUNG for financial support. M.T.G. acknowledges the 'Ministerio de Educación y Ciencia' and the Freiwillige Akademische Gesellschaft for financial support.

Author contributions

S.W., R.H. and M.T.G. carried out the experiments and conducted the analysis; S.G. synthesized the molecules; M.C., M.M. and C.S. designed the experiment, initiated the collaboration and supported the project in discussions; and S.W., C.S. and M.C. wrote the manuscript.

Author information

Reprints and permission information is available online at http://npg.nature.com/reprintsandpermissions/. Correspondence and requests for materials should be addressed to M.M.